AMERICAN SOCIETY FOR MICROBIOLOGY | Antimicrobial Agents and Chemotherapy®

MECHANISMS OF RESISTANCE

Kinetic Profile and Molecular Dynamic Studies Show that Y229W Substitution in an NDM-1/L209F Variant Restores the Hydrolytic Activity of the Enzyme toward Penicillins, Cephalosporins, and Carbapenems

Alessandra Piccirilli,[a] Fabrizia Brisdelli,[a] Massimiliano Aschi,[b] Giuseppe Celenza,[a] Gianfranco Amicosante,[a] Mariagrazia Perilli[a]

[a]Dipartimento di Scienze Cliniche Applicate e Biotecnologiche, Università degli Studi dell'Aquila, L'Aquila, Italy
[b]Dipartimento di Scienze Fisiche e Chimiche, Università degli Studi dell'Aquila, L'Aquila, Italy

ABSTRACT The New Delhi metallo-β-lactamase-1 (NDM-1) enzyme is the most common metallo-β-lactamase identified in many Gram-negative bacteria causing severe nosocomial infections. The aim of this study was to focus the attention on non-active-site residues L209 and Y229 of NDM-1 and to investigate their role in the catalytic mechanism. Specifically, the effect of the Y229W substitution in the L209F variant was evaluated by antimicrobial susceptibility testing, kinetic, and molecular dynamic (MD) studies. The Y229W single mutant and L209F-Y229W double mutant were generated by site-directed mutagenesis. The K_m, k_{cat}, and k_{cat}/K_m kinetic constants, calculated for the two mutants, were compared with those of (wild-type) NDM-1 and the L209F variant. Compared to the L209F single mutant, the L209F-Y229W double mutant showed a remarkable increase in k_{cat} values of 100-, 240-, 250-, and 420-fold for imipenem, meropenem, benzylpenicillin, and cefepime, respectively. In the L209F-Y229W enzyme, we observed a remarkable increase in k_{cat}/K_m of 370-, 140-, and 80-fold for cefepime, meropenem, and cefazolin, respectively. The same behavior was noted using the antimicrobial susceptibility test. MD simulations were carried out on both L209F and L209F-Y229W enzymes complexed with benzylpenicillin, focusing attention on the overall mechanical features and on the differences between the two systems. With respect to the L209F variant, the L209F-Y229W double mutant showed mechanical stabilization of loop 10 and the N-terminal region. In addition, Y229W substitution destabilized both the C-terminal region and the region from residues 149 to 154. The epistatic effect of the Y229W mutation jointly with the stabilization of loop 10 led to a better catalytic efficiency of β-lactams. NDM numbering is used in order to facilitate the comparison with other NDM-1 studies.

KEYWORDS NDM, enzyme kinetics, metallo-β-lactamases

Metallo-β-lactamases (MBLs) are zinc-dependent enzymes which represent the newest generation of broad-spectrum β-lactamases able to inactivate almost all classes of β-lactams. Based on their protein sequence similarities, three different lineages have been characterized, subclasses B1, B2, and B3 (1). Among subclass B1, New Delhi metallo-β-lactamase-1 (NDM-1) is one of the most diffused carbapenemases. This feature is due to its ability to hydrolyze all β-lactams (with the exception of monobactams), including the last-resort carbapenems. The prevalence of NDM producers was detected mainly in China and India but also in many European countries (2). NDM-1 was first identified in a multidrug-resistant *Klebsiella pneumoniae* strain isolated from a Swedish patient (3). To date, NDM-1 and its variants have been found in *Enterobacteriaceae*, including *Escherichia coli*, *Proteus mirabilis*, *K. pneumoniae*, and

Citation Piccirilli A, Brisdelli F, Aschi M, Celenza G, Amicosante G, Perilli M. 2019. Kinetic profile and molecular dynamic studies show that Y229W substitution in an NDM-1/L209F variant restores the hydrolytic activity of the enzyme toward penicillins, cephalosporins, and carbapenems. Antimicrob Agents Chemother 63:e02270-18. https://doi.org/10.1128/AAC.02270-18.

Address correspondence to Mariagrazia Perilli, perilli@univaq.it.

Received 27 October 2018
Returned for modification 5 December 2018
Accepted 23 January 2019
Accepted manuscript posted online 28 January 2019
Published 27 March 2019

Citrobacter koseri (4–7), as well as in nonfermenters such as *Pseudomonas aeruginosa* and *Acinetobacter baumannii* (8). Generally, these bacteria are highly resistant to several classes of antibiotics, including carbapenems, fluoroquinolones, and aminoglycosides (9, 10). The rapid spread of NDM-1 and NDM-1 variants is the result of the association of bla_{NDM} genes in complex mobile elements with successful plasmid scaffolds (11–13). The worldwide dissemination of NDM-producing *Enterobacteriaceae* is also linked to the huge reservoir represented by Indian subcontinent and Balkan countries (14). However, the clinical success of NDM enzymes is attributed as well to the fact that NDM-1, in Gram-negative bacteria, is a lipidated membrane-anchored enzyme (15). In fact, in these bacteria, NDM-1 is secreted in outer membrane vesicles, which increases the stability of the enzyme (15). The bla_{NDM} genes have evolved over time, and 21 NDM variants, differing from each other by a few amino acids, have been identified. In clinical isolates, the most frequent amino acid substitution found in NDM variants is M154L, present in a single or double mutant (NDM-4, NDM-5, NDM-7, NDM-8, NDM-12, NDM-13, and NDM-15). In many variants, D130 is replaced by a residue of asparagine (NDM-7) or glycine (NDM-8 and NDM-14) also in combination with M154L (NDM-7 and NDM-8). Single substitutions P28A, D95N, A233V, and R264H are present in NDM-2, NDM-3, NDM-6, and NDM-16, respectively (16, 17).

NDM-1 is a subclass B1 metallo-β-lactamase that works with two zinc ions for catalysis. The two zinc ions are coordinated by six conserved residues and one water molecule or hydroxide moiety (18). The Zn1 ligands are H120 (H116), H122 (H118), and H189 (H196), and the Zn2 ligands are D124 (D120), C208 (C221), and H250 (H263) (BBL numbering in parentheses). The active site of NDM-1 is a hydrophobic cavity which includes five loops playing an important role in the coordination of zinc ions, stability, and substrate binding of the enzyme. Two loops, loop 3 (roughly residues M67 to G73) and loop 10 (roughly residues I210 to A230) are able to correctly orient substrates within the active site (19–22). However, to make possible substrate hydrolysis, the active site needs both stability and flexibility. Residues within loop 6 and loop 10 are involved in the flexibility of the NDM-1 active site (19). Specifically, Y229 (Y244 in BBL numbering) and K125 (K121 in BBL numbering) residues play an important role in stabilizing loop 10 and loop 6, respectively (19). W229 is generally found in subclass B1 MBLs, such as VIM-2, VIM-4, BcII, and IMP-1. In NDM-1, residue Y229 is not in direct contact with substrate or zinc ions; however, the Y229W substitution results in a more active enzyme (23). Especially, Y229 forms hydrophobic contacts with several amino acids, including L209, which forms also hydrogen bonds with the aforementioned residue (23). The replacement of L209F causes a drastic reduction in β-lactamase activity toward penicillins, cephalosporins, and carbapenems (24). The aim of the present study was to evaluate, by kinetic analysis and molecular dynamic (MD) simulations, the effect of the Y229W substitution on the L209F variant. NDM numbering is used through the paper in order to facilitate the comparison with other NDM-1 studies.

RESULTS

Site-directed mutagenesis and antimicrobial susceptibility testing. Y229W and L209F-Y229W mutants were generated by site-directed mutagenesis using pFM-NDM-1 (25) and pET-24-L209F plasmids (20) as the templates, respectively. In order to obtain a large amount of these enzymes, both mutated genes (bla_{Y229W} and $bla_{L209F\text{-}Y229W}$), without signal peptide, were cloned into pET-24a(+) vector. First, the antimicrobial susceptibilities of the four enzymatic systems (NDM-1, L2019F, Y229W, and L209F-Y229W) were investigated versus a large panel of β-lactams (Table 1). MIC data obtained for *E. coli*/pET-24-Y229W and *E. coli*/pET-24-L209F-Y229W were compared with those of *E. coli*/pET-24-NDM-1 and *E. coli*/pET-24-L209F. As with NDM-1 and L209F mutant enzymes, the Y229W mutation confers resistance to all β-lactams tested, with the exception of cefoxitin (MIC, 8 μg/ml). Similarly, *E. coli*/pET-24-L209F-Y229W was resistant to all β-lactams, with MIC values slightly lower than those observed for *E. coli*/pET-24-NDM-1 and *E. coli*/pET-24-Y229W. Compared with *E. coli*/pET-24-NDM-1, the

TABLE 1 Antimicrobial susceptibilities of *E. coli* BL21(DE3)-CodonPlus carrying bla_{NDM-1}, $bla_{NDM-L209F}$, $bla_{NDM-Y229W}$, and $bla_{NDM-L209F-Y229W}$

	MIC (μg/ml) by *E. coli* strain				
β-Lactam	*E. coli*/pET-24 NDM-1	*E. coli*/pET-24 L209F	*E. coli*/pET-24 Y229W	*E. coli*/pET-24 L209F-Y229W	*E. coli*/pET-24
Imipenem	>64	0.25	>64	64	0.5
Meropenem	>64	<0.0625	>64	>64	0.5
Cefazolin	>128	4	>128	64	<0.0625
Cefotaxime	128	1	>128	32	<0.0625
Ceftazidime	>128	16	>128	32	<0.0625
Cefoxitin	8	8	8	4	0.125
Cefepime	32	<0.0625	16	16	<0.0625
Benzylpenicillin	>256	64	>256	>256	0.5
Carbenicillin	>256	64	>256	128	0.5

E. coli/pET-24-L209F strain showed susceptibility to carbapenems and cephalosporins, and it was resistant only to benzylpenicillin and carbenicillin.

Kinetic analysis of Y229W and L209F-Y229W enzymes. The Y229W (single mutant) and L209F-Y229W (double mutant) enzymes were purified (>95% pure) and used to determine the steady-state kinetic parameters toward several β-lactams. Table 2 shows the K_m, k_{cat}, and k_{cat}/K_m values for the NDM-1, L209F, Y229W, and L209F-Y229W enzymes. Kinetic data reported for NDM-1 (25, 26) and L209F (24) enzymes were from our previous studies. Compared with NDM-1, the Y229W single mutant showed a remarkable increase in k_{cat} values for benzylpenicillin, carbenicillin, meropenem, and cefazolin but not for imipenem and cefepime. For all β-lactams reported, in the case of Y229W mutant, the K_m values were higher than that calculated for NDM-1. Indeed, k_{cat}/K_m values for imipenem and cefepime were 4- and 18-fold lower than that of NDM-1 due to a reduction of k_{cat} and an increase in K_m values. Regarding imipenem, the Y229W mutant showed k_{cat} and k_{cat}/K_m values lower than those of NDM-1. On the contrary, meropenem exhibited k_{cat} and k_{cat}/K_m values 11- and 3-fold higher than that of NDM-1. With respect to the NDM-1 wild type, the Y229W mutant showed an increase in k_{cat} and k_{cat}/K_m values for cefazolin. Concerning cefepime, the Y229W mutant exhibited lower k_{cat} value but higher k_{cat}/K_m values than those for NDM-1 (Table 2). In the L209F mutant, a drastic reduction in activity toward penicillins, cefazolin, and carbapenems was measured (24). The K_m values of L209F-Y229W for penicillins were higher than that of L209F single mutant but comparable to the values calculated for NDM-1. The L209F-Y229W mutant showed k_{cat} values higher than those calculated for L209F and, in the case of benzylpenicillin and meropenem, even higher than those of NDM-1. Indeed, k_{cat} values for carbenicillin and benzylpenicillin increased 70- and 250-fold, respectively. The catalytic efficiencies of the L209F-Y229W double mutant for carbenicillin and benzylpenicillin were similar to those of NDM-1 but about 5-fold higher than those for the L209F variant (Table 3). Concerning imipenem, the K_m values were about 3-fold higher than those calculated for NDM-1 and the L209F mutant. In

TABLE 2 Determination of kinetic parameters of NDM-1, L209F, Y229W, and L209F-Y229W enzymes

	Values by enzyme[a]											
	NDM-1[b]			L209F mutant[c]			Y229W mutant[d]			L209F-Y229W mutant[d]		
Substrate	K_m (μM)	k_{cat} (s^{-1})	k_{cat}/K_m ($\mu M^{-1}\ s^{-1}$)	K_m (μM)	k_{cat} (s^{-1})	k_{cat}/K_m ($\mu M^{-1}\ s^{-1}$)	K_m (μM)	k_{cat} (s^{-1})	k_{cat}/K_m ($\mu M^{-1}\ s^{-1}$)	K_m (μM)	k_{cat} (s^{-1})	k_{cat}/K_m ($\mu M^{-1}\ s^{-1}$)
Benzylpenicillin	210 ± 15	105	0.42	7 ± 0.5	1.00	0.14	841 ± 35	552 ± 5	0.66	378 ± 20	250 ± 4	0.66
Carbenicillin	285 ± 5	108	0.38	20 ± 3	1.40	0.07	1,219 ± 200	1,258 ± 8	1.03	285 ± 16	94 ± 2	0.33
Cefazolin	20 ± 1	42	2.10	16 ± 2	0.34	0.021	48 ± 2	191 ± 4	3.98	15 ± 1	25 ± 1	1.66
Imipenem	35 ± 1	64	1.83	33 ± 5	0.55	0.017	81 ± 3	38 ± 1	0.47	120 ± 9	55 ± 3	0.46
Meropenem	80 ± 2	75	0.94	50 ± 1	0.86	0.017	259 ± 18	820 ± 6	3.17	88 ± 4	208 ± 7	2.36
Cefepime	35 ± 5	13	0.37	99 ± 3	0.019	1.9×10^{-4}	117 ± 8	2.5 ± 0.2	0.02	113 ± 7	8 ± 0.5	0.07

[a]Each kinetic value represents the mean of the results of three different measurements; the error rate was below 10%.
[b]Data from Marcoccia et al. (24–26).
[c]Data from Marcoccia et al. (24).
[d]Data from this study.

TABLE 3 k_{cat} and k_{cat}/K_m ratio calculated for L209F-Y229W double mutant versus L209F mutant enzyme

Substrate	k_{cat} ratio for L209F-Y229W mutant vs L209F mutant	k_{cat}/K_m ratio for L209F-Y229W mutant vs L209F mutant
Benzylpenicillin	250	5
Carbenicillin	70	5
Imipenem	100	27
Meropenem	240	140
Cefazolin	75	80
Cefepime	420	370

Table 3, we compared the k_{cat} and k_{cat}/K_m values of the L209F-Y229W mutant versus the L209F mutant. A remarkable increase in these values was observed in all β-lactams tested. In particular, compared to the L209F mutant, the L209F-Y229W double mutant showed for imipenem and meropenem increases of about 100- and 240-fold in the k_{cat} values and 27- and 140-fold in the k_{cat}/K_m values, respectively.

Molecular dynamic simulations. The identification of the key factors at the molecular level of the positive effects of the Y229W substitution in the L209F mutant enzyme is a prohibitive task from a computational point of view. In fact, the complexity of the enzyme systems is too high to reduce the experimental observation (i.e., the result of many events distributed in huge time and space domain at atomistic level) to a single and point-like origin. For this reason, we performed molecular dynamics (MD) simulations on the L209F and L209F-Y229W enzymes complexed with benzylpenicillin, focusing attention on the overall mechanical features and on the differences between the two systems. In Fig. 1, a comparison of Cα root mean square fluctuation (RMSF) of the two complexed enzymes is depicted. The RMSF pattern is not dramatically different in the systems, indicating that, as expected, both of the enzymes maintain the overall structural features without undergoing unfolding processes at least within the 100.0-ns simulations. At the same time, three sharp and important differences were observed. In particular, the L209F-Y229W double mutant compared to the L209F mutant revealed (i) mechanical destabilization (i.e., RMSF increase) of the region 149 to 154, (ii) mechanical stabilization (i.e., RMSF decrease) of the loop 10 and N-terminal regions, and (iii) mechanical destabilization of the C-terminal region. These mechanical differences,

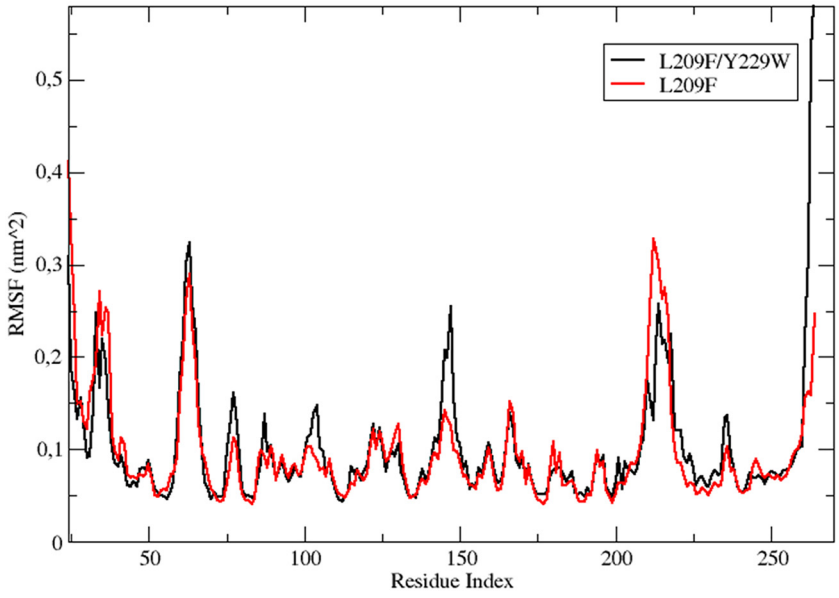

FIG 1 Comparison of the Cα root mean square fluctuation (RMSF) of the L209F-Y229W mutant (black) with that of the L209F mutant (red).

concerning crucial regions of the enzymes, could be related to what was observed experimentally. Subsequently, we have undergone a more detailed analysis of the local interactions experienced by the residues F209 and W229 in both mutants (L209F and L209F-Y229W). This analysis does not reveal dramatic differences. In fact, in the L209F-Y229W enzyme, the contacts appear, within the margin of error, similar to those of the L209F mutant. However, we also observe a systematic increase in the standard deviation, indicating that Y229W replacement induces a local mechanical stabilization also in the region near the 209 residue.

DISCUSSION

In the present paper, we have investigated by molecular dynamics and kinetic studies the interaction between residues 209 and 229 in New Delhi metallo-β-lactamase 1 and their involvement in hydrolytic activity. Leucine 209 in NDM-1 is located in loop 10, in the "second-sphere residues" outside the active site of the enzyme. Residue 209 is positioned just before Zn2 binding ligand C208 (C221 in BBL numbering). Crystal studies on NDM-1 have established that L209 forms hydrophobic interactions with the Y229 residue (18–23). In addition, the Y229 residue plays an important role in loop 10 stability, forming hydrophobic interactions not only with L209 but also with neighboring residues, such as L269, L218, and L221. These hydrophobic interactions contribute to stabilization and orientation of loop 10 with respect to the C-terminal β-sheet (23). In our previous paper, we showed that the L209F substitution in an NDM-1 leads to a drastic reduction in k_{cat} and k_{cat}/K_m values toward carbapenems (imipenem and meropenem), penicillins, and cephalosporins (24). In the case of the L209F mutant, we have demonstrated that the presence of F209 perturbs the interactions of this residue with neighboring residues, and a major fluctuation of loop 10 was observed with respect to NDM-1 (24). In particular, in the NDM-1 enzyme, the L209 residue interacts with Y229 by hydrogen bonds. Differently from other subclass B1 MBLs, which have tryptophan at position 229, NDM-1 employs a tyrosine residue. Chen et al. demonstrated that the Y229W substitution in NDM-1 improves the catalytic efficiency toward some β-lactams, especially benzylpenicillin, cefuroxime, and meropenem (23). Herein, we generated a double mutant of the NDM-1 enzyme, L209F-Y229W, to verify our hypothesis that the addition of the Y229W substitution could be able to restore the hydrolytic activity of the L209F mutant enzyme. In order to investigate the effect of Y229W replacement in the L209F enzyme, kinetic analysis and molecular dynamics simulations have been performed. Our results showed that the replacement Y229W changes substantially the kinetic behavior of the L209F enzyme. Compared with L209F, in the L209F-Y229W enzyme, we observed a remarkable increase in k_{cat} values of 100-, 240-, 250-, and 420-fold for imipenem, meropenem, benzylpenicillin, and cefepime, respectively. The K_m values for benzylpenicillin and carbenicillin calculated for the double mutant were 54- and 14-fold higher than that of L209F but similar to that for NDM-1. Compared to the L209F mutant, the L209F-Y229W double mutant seems to have lower affinity for penicillins. When introduced into the L209F single mutant, the Y229W mutation was able to restore the activity of the enzyme that showed high catalytic efficiency values. This is particularly true for cefepime, meropenem, and cefazolin, to which we observed an increase in k_{cat}/K_m values of 370-, 140-, and 80-fold, respectively. Molecular dynamics simulations were performed on the L209F and L209F-Y229W mutants, complexed with benzylpenicillin, in order to observe structural and dynamic differences induced by amino acid substitutions. The enzyme internal mobility, based on root mean square fluctuation (RMSF), is characterized by fluctuations in different regions, including the loop 10, N-terminal, C-terminal, and 149 to 154 regions. An evident effect was observed at loop 10. Compared to the single mutant, the L209F-Y229W double mutant showed a decrease in RMSF peak resulting in better mechanical stabilization of loop 10. Fluctuations observed in the two enzymes complexed with benzylpenicillin could probably affect the affinity (K_m values) versus some β-lactams. In the L209F-Y229W double mutant, we noticed a decrease in RMSF peak in loop 10 (residues F209 to A230), resulting in better mechanical stabilization of

loop 10. Undoubtedly, these fluctuations could perturb the zinc ion geometry, resulting in an improvement in hydrolytic activity. In a recent paper, Zhang and coworkers demonstrated that the modulation of Zn1-to-Zn2 distance affects the enzymatic activity of NDM-1 (27). In particular, they have been underlined that a bigger fluctuation of the active site corresponds to a shorter distance between Zn1 and Zn2, favoring higher enzymatic activity. However, the mechanism through which NDM-1 hydrolyzes substrate is complex. As demonstrated by several authors, the enzyme-substrate reaction proceeds by almost two reactive intermediates (28, 29). In MBLs, the main "protagonist" of substrate binding is Zn2. We speculate that the enhancement of enzymatic activity of the L209F-Y229W double mutant with respect to the L209F mutant enzyme could be due to fluctuations generated in non-active-site regions, which might modify the Zn1-to-Zn2 distance and the reactivity of Zn2.

Moreover, the enhancement of the hydrolytic activity of the L209F-Y229W mutant could be also attributable to the epistatic effect of the Y229W mutation that involved enzyme catalysis. The epistatic effect of some mutations was also ascertained in the BcII enzyme (30, 31). Compared to NDM-1, the L209F mutation leads to a decrease in activity; on the contrary, the Y229W single mutant showed an increase in catalytic efficiency toward penicillins, cefazolin, and meropenem but not for imipenem and cefepime. The interaction of F209 and W229 not only restored the activity of the enzyme (double mutant) but, in the case of benzylpenicillin and meropenem, the L209F-Y229W mutant showed an increase in k_{cat} and k_{cat}/K_m parameters with respect to NDM-1. The Y229W mutation is responsible for a large increase in catalytic efficiency. A noteworthy increase in resistance versus all β-lactams tested was observed in *E. coli*/pET-24-L209F-Y229W with respect to *E. coli*/pET-24-L209F. Specifically, in the L209F-Y229W mutant, an increase of MIC values was observed, in particular, for meropenem and cefepime. In conclusion, we stated that several both loop fluctuations and the epistatic effect of the Y229W mutation could have contributed to the restoration of β-lactam activity in the L209F mutant enzyme.

MATERIALS AND METHODS

Site-directed mutagenesis and cloning. The NDM-1 Y229W and L209F-Y229W mutants were generated by site-directed mutagenesis (32) from pFM-NDM-1 and pET-24-L209F, which contain bla_{NDM} without N-terminal lipidation signal (first 35 amino acids) (24, 25). In order to amplify the entire gene, the NDM_for (5′-GGGGG**CATATG**GGTGAAATCCGCCCGA) and NDM_rev (5′-GGGGG**CTCGAG**TCAGCGCAGCT TGTCGGC) primers were used (restriction site sequences are in bold). For site-directed mutagenesis, the Y229W_for (5′-ACTGAGCACTGGGCCGCGTCA) and Y229W_rev (5′-TGACGCGGCCCAGTGCTCAGT) primers were used (the mutated sequence is underlined). DNA sequences coding for NDM variants were cloned into the pET-24a(+) overexpression vector digested with NdeI and XhoI restriction enzymes. The authenticity of NDM variants was confirmed by sequencing recombinant plasmids using an automated sequencer (ABI Prism 3500; Life Technologies, Monza, Italy). The *E. coli* NovaBlue strain was used for the initial cloning as a nonexpression host. The *E. coli* BL21(DE3)-CodonPlus strain was used for overexpression of the bla_{NDM} mutants.

Expression and purification of Y229W and L209F-Y229W enzymes. *E. coli* BL21(DE3)-CodonPlus cells harboring bla_{Y229W} and $bla_{L209F\text{-}Y229W}$ were grown in 1 liter of tryptic soy broth (TSB) medium with 50 μg/ml kanamycin at 37°C in an orbital shaker (180 rpm). Each culture was grown to achieve an A_{600} of approximately 0.5, and 0.4 mM isopropyl-β-D-thiogalactoside (IPTG) was added. After the addition of IPTG, the cultures were incubated for 16 h at 22°C under aerobic conditions. Cells were harvested by centrifugation at 8,000 rpm for 10 min at 4°C and washed twice with 25 mM Tris-HCl buffer (pH 7.6) (buffer A). Crude enzymes were obtained by sonication in ice (5 cycles at 60 W with 2 min of break). The lysate was centrifuged at 22,000 rpm for 60 min, and the cleared supernatant was recovered and loaded onto a Q Sepharose Fast Flow column equilibrated with buffer A. The column was extensively washed to remove unbound proteins, and the metallo-β-lactamase was eluted with a linear gradient of 25 mM Tris-HCl (pH 7.6) plus 1 M NaCl (buffer B). The fractions containing β-lactamase activity were pooled, concentrated 20-fold using an Amicon concentrator (YM 10 membrane; Millipore, Bedford, MA, USA), dialyzed in 30 mM morpholineethanesulfonic acid (MES [pH 5.9]), and loaded onto a Mono S column equilibrated with the same buffer. The active fractions were collected during the elution process and then dialyzed in 20 mM HEPES buffer (pH 7.0) for kinetic experiments.

Antibiotics. Meropenem was obtained from AstraZeneca (Milan, Italy). Imipenem was obtained from Merck Sharp & Dohme (Rome, Italy). The other antimicrobial agents used in this study were purchased from Sigma-Aldrich (Milan, Italy). The molar extinction coefficients and wavelengths used in the assay were imipenem $\Delta\varepsilon_{300}$, $-9{,}000\ M^{-1}\ cm^{-1}$; meropenem $\Delta\varepsilon_{297}$, $-6{,}500\ M^{-1}\ cm^{-1}$; cefepime $\Delta\varepsilon_{260}$, $-10{,}000\ M^{-1}\ cm^{-1}$; cefazolin $\Delta\varepsilon_{260}$, $-7{,}400\ M^{-1}\ cm^{-1}$; carbenicillin $\Delta\varepsilon_{235}$, $-780\ M^{-1}\ cm^{-1}$; and benzylpenicillin $\Delta\varepsilon_{235}$, $-775\ M^{-1}\ cm^{-1}$.

Determination of kinetic parameters. Steady-state kinetic experiments were performed following the hydrolysis of the β-lactams at 25°C in HEPES 20 mM (pH 7.0) plus 20 μM $ZnCl_2$. The data were collected with a Lambda 25 spectrophotometer (PerkinElmer Italia, Monza, Italy). Kinetic parameters were determined under initial-rate conditions using the GraphPad Prism 6 software to generate Michaelis-Menten curves or by analyzing the complete hydrolysis time courses (33, 34). Each kinetic value represents the mean of the results from three different measurements; the error rate was below 10%. To calculate k_{cat} values, we used the theoretical molecular weight of 25,605.87 Da, assuming cleavage of signal peptide at residue G29 (G24 according to BBL standard numbering), as predicted from SignalP 4.0 (35).

Antimicrobial susceptibility. The phenotypic profile has been characterized by a microdilution method using a bacterial inoculum of 5×10^5 CFU/ml according to Clinical and Laboratory Standards Institute (CLSI) performance standards (36). The *E. coli* BL21(DE3)-CodonPlus strains used for MIC experiments were those with recombinant plasmids without signal peptide. Resistance breakpoints were determined according to CLSI guidelines (37).

Computational details. All the simulations were carried out using the Gromacs package, version 4.5.5 (38). The charges of the substrate (benzylpenicillin) and active site were calculated using standard fitting procedures with the program Gaussian 09 (39). For the simulations, the enzyme was inserted in a cubic box filled with 7,965 molecules of water described with the simple point charge (spc) model (40). The dimensions of the box were adjusted to correctly reproduce the density of the system at 298 K and 10^5 Pa of pressure, as previously described (41). The simulations were performed in the NVT ensemble and extended for 100.0 ns.

A time step of 2.0 fs was employed in conjunction with a standard protocol, where after an initial energy minimization, the system was gradually heated from 50 to 250 K using short (20-ps) MD simulations. Finally, a further preequilibration of the system, arrived at 298 K, was carried out by running 5.0 ns of MD simulation in all the systems. Note that all these equilibration trajectories were only utilized for obtaining the initial configuration and hence disregarded by the following analysis. The temperature was kept constant using the velocity rescaling procedure. The LINCS algorithm was employed to constrain all bond lengths (42). Long-range electrostatic interactions were computed by the Particle mesh Ewald method with 34 wave vectors in each dimension and a fourth-order cubic interpolation, and a cutoff 1.1 nm was used (43).

The starting coordinates of the simulations were obtained by modifying the crystal structure of NDM-1 coordinated to hydrolyzed benzylpenicillin (here termed BzP) taken from the Protein Data Bank (PDB ID 4EYF) (20, 44). Based on previous experimental and computational studies (20), we explicitly bound the BzP carbonyl group to Zn1 and the BzP amide nitrogen and carboxylate group to Zn2. The mutants were obtained with the program Molden (45).

ACKNOWLEDGMENTS

We thank Anna Toso (Toronto Catholic District School Board, Toronto, Canada) for the language revision of the manuscript.

We declare no conflicts of interest.

REFERENCES

1. Garau G, Garcia-Saez I, Bebrone C, Anne C, Mercuri P, Galleni M, Frere J-M, Dideberg O. 2004. Update of the standard numbering scheme for class B β-lactamases. Antimicrob Agents Chemother 48:2347–2349. https://doi.org/10.1128/AAC.48.7.2347-2349.2004.
2. Khan AU, Maryam L, Zarrilli R. 2017. Structure, genetics and worldwide spread of New Delhi metallo-β-lactamase (NDM): a threat to public health. BMC Microbiol 17:101. https://doi.org/10.1186/s12866-017-1012-8.
3. Yong D, Toleman MA, Giske CG, Cho HS, Sundman K, Lee K, Walsh TR. 2009. Characterization of a new metallo-β-lactamase gene, bla_{NDM-1}, and a novel erythromycin esterase gene carried on a unique genetic structure in *Klebsiella pneumoniae* sequence type 14 from India. Antimicrob Agents Chemother 53:5046–5054. https://doi.org/10.1128/AAC.00774-09.
4. Rahman M, Mukhopadhyay C, Rai RP, Singh S, Gupta S, Singh A, Pathak A, Prasad KN. 2018. Novel variant NDM-11 and other NDM-1 variants in multidrug resistant *Escherichia coli* from South India. J Glob Antimicrob Resist 14:154–157. https://doi.org/10.1016/j.jgar.2018.04.001.
5. Kanzari L, Ferjani S, Saidani M, Hamzaoui Z, Jendoubi A, Harbaoui S, Ferjani A, Rehaiem A, Boutiba Ben Boubaker I, Slim A. 2018. First report of extremely drug resistant *Proteus mirabilis* isolate carrying plasmid-mediated bla_{NDM-1} in a Tunisian intensive care unit. Int J Antimicrob Agents 52:906–909. https://doi.org/10.1016/j.ijantimicag.2018.06.009.
6. Solgi H, Badmasti F, Giske CG, Aghamohammad S, Shahcheraghi F. 2018. Molecular epidemiology of NDM-1- and OXA-48-producing *Klebsiella pneumoniae* in an Iranian hospital: clonal dissemination of ST11 and ST893. J Antimicrob Chemother 73:1517–1524. https://doi.org/10.1093/jac/dky081.
7. Kocsis E, Gužvinec M, Butić I, Krešić S, Crnek SŠ, Tambić A, Cornaglia G, Mazzariol A. 2016. bla_{NDM-1} carriage on IncR plasmid in Enterobacteriaceae strains. Microb Drug Resist 22:123–128. https://doi.org/10.1089/mdr.2015.0083.
8. Tanner WD, Atkinson RM, Goel RK, Toleman MA, Benson LS, Porucznik CA, VanDerslice JA. 2017. Horizontal transfer of the bla_{NDM-1} gene to *Pseudomonas aeruginosa* and *Acinetobacter baumannii* in biofilms. FEMS Microbiol Lett 1:364. https://doi.org/10.1093/femsle/fnx048.
9. Kumarasamy KK, Toleman MA, Walsh TR, Bagaria J, Butt F, Balakrishnan R, Chaudhary U, Doumith M, Giske CG, Irfan S, Krishnan P, Kumar AV, Maharjan S, Mushtaq S, Noorie T, Paterson DL, Pearson A, Perry C, Pike R, Rao B, Ray U, Sarma JB, Sharma M, Sheridan E, Thirunarayan MA, Turton J, Upadhyay S, Warner M, Welfare W, Livermore DM, Woodford N. 2010. Emergence of a new antibiotic resistance mechanism in India, Pakistan, and the UK: a molecular, biological, and epidemiological study. Lancet Infect Dis 10:597–602. https://doi.org/10.1016/S1473-3099(10)70143-2.
10. Gamal D, Fernández-Martínez M, Salem D, El-Defrawy I, Montes LÁ, Ocampo-Sosa AA, Martínez-Martínez L. 2016. Carbapenem-resistant *Klebsiella pneumoniae* isolates from Egypt containing bla_{NDM-1} on IncR plasmids and its association with rmtF. Int J Infect Dis 43:17–20. https://doi.org/10.1016/j.ijid.2015.12.003.
11. Bonnin RA, Poirel L, Carattoli A, Nordmann P. 2012. Characterization of an IncFII plasmid encoding NDM-1 from *Escherichia coli* ST131. PLoS One 7:e34752. https://doi.org/10.1371/journal.pone.0034752.
12. Villa L, Poirel L, Nordmann P, Carta C, Carattoli A. 2012. Complete sequencing of an IncH plasmid carrying the bla_{NDM-1}, $bla_{CTX-M-15}$ and

qnrB1 genes. Antimicrob Chemother 67:1645–1650. https://doi.org/10.1093/jac/dks114.
13. Villa L, Guerra B, Schmoger S, Fischer J, Helmuth R, Zong Z, García-Fernández A, Carattoli A. 2015. IncA/C plasmid carrying bla_{NDM-1}, bla_{CMY-16}, and fosA3 in a *Salmonella enterica* serovar Corvallis strain isolated from a migratory wild bird in Germany. Antimicrob Agents Chemother 59:6597–6600. https://doi.org/10.1128/AAC.00944-15.
14. Dortet L, Poirel L, Nordmann P. 2014. Worldwide dissemination of the NDM-type carbapenemases in Gram-negative. Biomed Res Int 2014:249856. https://doi.org/10.1155/2014/249856.
15. González LJ, Bahr G, Nakashige TG, Nolan EM, Bonomo RA, Vila AJ. 2016. Membrane-anchoring stabilizes and favors secretion of New Delhi Metallo-β-lactamase. Nat Chem Biol 12:516–522. https://doi.org/10.1038/nchembio.2083.
16. Bahr G, Vitor-Horen L, Bethel CR, Bonomo RA, González LJ, Vila AJ. 2018. Clinical evolution of New Delhi metallo-β-lactamase (NDM) optimizes resistance under Zn(II) deprivation. Antimicrob Agents Chemother 62:e01849-17. https://doi.org/10.1128/AAC.01849-17.
17. Cheng Z, Thomas PW, Ju L, Bergstrom A, Mason K, Clayton D, Miller C, Bethel CR, VanPelt J, Tierney DL, Page RC, Bonomo RA, Fast W, Crowder MW. 2018. Evolution of New Delhi metallo-β-lactamase (NDM) in the clinic: effects of NDM mutations on stability, zinc affinity, mono-zinc activity. J Biol Chem 293:12606–12618. https://doi.org/10.1074/jbc.RA118.003835.
18. Kim Y, Cunningham MA, Mire J, Tesar C, Sacchettini J, Joachimiak A. 2013. NDM-1, the ultimate promiscuous enzyme: substrate recognition and catalytic mechanism. FASEB J 27:1917–1927. https://doi.org/10.1096/fj.12-224014.
19. Zhang H, Hao Q. 2011. Crystal structure of NDM-1 reveals a common β-lactam hydrolysis mechanism. FASEB J 25:2574–2582. https://doi.org/10.1096/fj.11-184036.
20. King D, Strynadka N. 2011. Crystal structure of New Delhi metallo-β-lactamase reveals molecular basis for antibiotic resistance. Protein Sci 20:1484–1491. https://doi.org/10.1002/pro.697.
21. Guo Y, Wang J, Niu G, Shui W, Sun Y, Zhou H, Zhang Y, Yang C, Lou Z, Rao Z. 2011. A structural view of the antibiotic degradation enzyme NDM-1 from a superbug. Protein Cell 2:384–394. https://doi.org/10.1007/s13238-011-1055-9.
22. Khan S, Ali A, Khan AU. 2018. Structural and functional insight of New Delhi metallo-β-lactamase-1 variants. Future Med Chem 10:221–229. https://doi.org/10.4155/fmc-2017-0143.
23. Chen J, Chen H, Shi Y, Hu F, Lao X, Gao X, Zheng H, Yao W. 2013. Probing the effect of the non-active-site mutation Y229W in New Delhi metallo-β-lactamase-1 by site-directed mutagenesis, kinetic studies, and molecular dynamics simulations. PLoS One 8:e82080. https://doi.org/10.1371/journal.pone.0082080.
24. Marcoccia F, Leiros HKS, Aschi M, Amicosante G, Perilli M. 2018. Exploring the role of L209 residue in active site of NDM-1 a metallo-β-lactamase. PLoS One 13:e0189686. https://doi.org/10.1371/journal.pone.0189686.
25. Marcoccia F, Bottoni C, Sabatini A, Colapietro M, Mercuri PS, Galleni M, Kerff F, Matagne A, Celenza G, Amicosante G, Perilli M. 2016. Kinetic study of laboratory mutants of NDM-1 metallo-β-lactamase and the importance of an isoleucine at position 35. Antimicrob Agents Chemother 60:2366–2372. https://doi.org/10.1128/AAC.00531-15.
26. Marcoccia F, Mercuri PS, Galleni M, Celenza G, Amicosante G, Perilli M. 2018. A kinetic study of the replacement by site saturation mutagenesis of residue 119 in NDM-1 metallo-β-lactamase. Antimicrob Agents Chemother 62:02541-17. https://doi.org/10.1128/AAC.02541-17.
27. Zhang H, Ma G, Zhu Y, Zeng L, Ahmad A, Wang C, Pang B, Fang H, Zhao L, Hao Q. 2018. Active site conformational fluctuations promote the enzymatic activity of NDM-1. Antimicrob Agents Chemother 62:e01579-18. https://doi.org/10.1128/AAC.01579-18.
28. Lisa MN, Palacios AR, Aitha M, González MM, Moreno DM, Crowder MW, Bonomo RA, Spencer J, Tierney DL, Llarrull LI, Vila AJ. 2017. A general reaction mechanism for carbapenem hydrolysis by mononuclear and binuclear metallo-β-lactamases. Nature Commun 8:538. https://doi.org/10.1038/s41467-017-00601-9.
29. Feng H, Liu X, Wang S, Fleming J, Wang DC, Liu W. 2017. The mechanism of NDM-1 catalyzed carbapenem hydrolysis is distinct from that of penicillin or cephalosporin hydrolysis. Nat Commun 8:2242. https://doi.org/10.1038/s41467-017-02339-w.
30. Meini MR, Tomatis PE, Weinreich DM, Vila AJ. 2015. Quantitative description of a protein fitness landscape based on molecular features. Mol Biol Evol 32:1774–1787. https://doi.org/10.1093/molbev/msv059.
31. González MM, Abriata LA, Tomatis PE, Vila AJ. 2016. Optimization of conformational dynamics in an epistatic evolutionary trajectory. Mol Biol Evol 33:1768–1776. https://doi.org/10.1093/molbev/msw052.
32. Perilli M, Celenza G, De Santis F, Pellegrini C, Forcella C, Rossolini GM, Stefani S, Amicosante G. 2008. E240V substitution increases catalytic efficiency toward ceftazidime in a new natural TEM-type extended spectrum β-lactamase (TEM-149) from *Enterobacter aerogenes* and *Serratia marcescens* clinical isolates. Antimicrob Agents Chemother 52:915–919. https://doi.org/10.1128/AAC.01028-07.
33. Segel IH. 1976. Methods of plotting enzyme kinetics data, p 236–241. *In* Segel IH (ed), Biochemical calculations: how to solve mathematical problems in general biochemistry, 2nd ed. John Wiley & Sons, New York, NY.
34. Celenza G, Luzi C, Aschi M, Segatore B, Setacci D, Pellegrini C, Forcella C, Amicosante G, Perilli M. 2008. Natural D240G Toho-1 mutant conferring resistance to ceftazidime: biochemical characterization of CTX-M-43. J Antimicrob Chemother 62:991–997. https://doi.org/10.1093/jac/dkn339.
35. Nordahl Petersen T, Brunak S, von Heijne G, Nielsen H. 2011. SignalP 4.0: discriminating signal peptides from transmembrane regions. Nat Methods 8:785–786. https://doi.org/10.1038/nmeth.1701.
36. Clinical and Laboratory Standards Institute. 2018. Methods for dilution antimicrobial susceptibility tests for bacteria that grow aerobically; approved standard, 11th ed. CLSI document M07. Clinical and Laboratory Standards Institute, Wayne, PA.
37. Clinical and Laboratory Standards Institute. 2018. Performance standards for antimicrobial susceptibility testing, 28th ed. CLSI document M100. Clinical and Laboratory Standards Institute, Wayne, PA.
38. Van der Spoel D, Lindahl E, Hess B, Groenhof G, Mark AE, Berendsen HJC. 2005. GROMACS: fast, flexible and free. J Comput Chem 26:1701–1718. https://doi.org/10.1002/jcc.20291.
39. Frisch MJ, Trucks GW, Schlegel HB, Scuseria GE, Robb MA, Cheeseman JR, Scalmani G, Barone V, Mennucci B, Petersson GA, Nakatsuji H, Caricato M, Li X, Hratchian HP, Izmaylov AF, Bloino J, Zheng G, Sonnenberg JL, Hada M, Ehara M, Toyota K, Fukuda R, Hasegawa J, Ishida M, Nakajima T, Honda Y, Kitao O, Nakai H, Vreven T, Montgomery JA, Jr, Peralta JE, Ogliaro F, Bearpark M, Heyd JJ, Brothers E, Kudin KN, Staroverov VN, Kobayashi R, Normand J, Raghavachari K, Rendell A, Burant JC, Iyengar SS, Tomasi J, Cossi M, Rega N, Millam JM, Klene M, Knox JE, Cross JB, et al. 2009. Gaussian 09, Revision E.01, Gaussian, Inc., Wallingford, CT.
40. Berendsen JC, Postma JPM, van Gunsteren WF, Hermans J. 1981. Interaction models for water in relation to protein hydration, p 331. *In* Pullman B (ed), Intermolecular forces. Reidel, Dordrecht, the Netherlands.
41. Aschi M, D'Abramo M, Amadei A. 2016. Photoinduced electron transfer in a dichromophoric peptide: a numerical experiment. Theor Chem Acc 135:132. https://doi.org/10.1007/s00214-016-1881-1.
42. Hess B, Bekker H, Berendsen HJC, Fraaije JGEM. 1997. LINCS: a linear constraint solver for molecular simulations. J Comput Chem 18:1463. https://doi.org/10.1002/(SICI)1096-987X(199709)18:12<1463::AID-JCC4>3.3.CO;2-L.
43. Darden TA, York DM, Pedersen LG. 1993. Particle mesh Ewald: an N·log (N) method for Ewald sums in large systems. J Chem Phys 98:10089. https://doi.org/10.1063/1.464397.
44. King DT, Worrall LJ, Gruninger R, Strynadka NC. 2012. New Delhi metallo-β-lactamase: structural insights into β-lactam recognition and inhibition. J Am Chem Soc 134:11362–11365. https://doi.org/10.1021/ja303579d.
45. Schaftenaar G, Noordik JH. 2000. Molden: a pre- and post-processing program for molecular and electronic structures. J Comput Aided Mol Des 14:123–134. https://doi.org/10.1023/A:1008193805436.